

Rajul Rastogi^{1*} and Sujeet Kumar Jain²¹Teerthanker Mahaveer Medical College and Research Center, Moradabad, U.P, 244001 India²School of Medical Sciences & Research, Greater Noida, U.P, India**Dates:** Received: 29 February, 2016; Accepted: 25 May, 2016; Published: 28 May, 2016***Corresponding author:** Dr. Rajul Rastogi, Teerthanker Mahaveer Medical College and Research Center, Moradabad, UP, India, 244001, E-mail: eesharastogi@gmail.com

www.peertechz.com

Review Article

Imaging in Diabetes Mellitus

Type IV: Gestational Diabetes Mellitus or Diabetes Mellitus of Pregnancy

The above classification is relevant to imaging specialists as well, the type of DM (primary or secondary) will affect manifestations and the complications including their severity. It is of equal significance for those patients undergoing some interventional radiological procedure for diagnosis or treatment.

Cardiovascular system [1-7]

Cardiac involvement in diabetes mellitus occurs in the form of coronary artery sclerosis or atherosclerosis, congestive cardiac failure, acute ischemia or infarction.

In acute ischemia or infarction, role of scintigraphy (technetium thallium scan), SPECT and cardiac MRI is well documented. These modalities are useful in detecting at-risk, ischemic, infarcted, nonviable and scarred regions of myocardium. The abnormal area appears as a region of hypoperfusion or cold spot with or without dyskinesia. 2D- echocardiography (ECHO) is very useful in assessing the status of cardiac chambers and flow through the valves. Pericardial effusion can also be detected with high sensitivity by ECHO. Radiograph of chest is very helpful in the assessment of the status of pulmonary parenchyma & vasculature and presence of pleural effusion. Pleural effusions can be detected with higher sensitivity with high resolution ultrasonography of the pleural spaces. Radiograph of chest may reveal signs of pulmonary venous hypertension in the form of Kerley B lines especially at the bases, upper lobe blood diversion, alveolar & interstitial opacities and in severe cases, hilar and perihilar pneumonic consolidation in *bat-wing pattern*.

In congestive cardiac failure, besides chest radiograph, ultrasonography of the abdomen is very useful in assessing the back pressure changes as depicted by the dilatation and engorgement of the hepatic veins and inferior vena cava. There may be associated hepatomegaly and fluid in the serous cavities including pleural, peritoneal and pericardial cavities.

Asymptomatic coronary artery disease (CAD) is common in NIDDM patients. Noninvasive detection of carotid intima-media thickening by ultrasound has been accepted as a surrogate marker of the increased risk of subclinical CAD in diabetic patients. Coronary arteriosclerosis and atherosclerosis can be well studied with CT angiography or invasive coronary angiography. Though, both modalities can give reliable information regarding the degree of stenosis, yet CT angiography scores over invasive angiography in revealing information regarding the walls of arteries & nature of plaque while the latter is more accurate in detecting degree of stenosis and collateral circulation. Atherosclerotic plaques appear hypodense on CT scans due to their lipid content while calcium appears hyperdense with CT – attenuation values of greater than

Review

Diabetes mellitus [DM] is the commonest endocrine disorder encountered in the clinical practice. It in fact, comprises of multiple disorders that manifest in the form of hyperglycemia. It is a multisystem disorder with pathophysiologic changes occurring in almost all the major systems and organs of the human body resulting in serious physical and mental disturbances and also posing tremendous burden on the health care resources of the country. The common sites of involvement include cardiovascular system, nervous system (central and peripheral), eyes, gastrointestinal system, genitourinary system, nasal and paranasal sinus region, hepatopancreatobiliary system, etc. Radiological manifestations are directly proportional to the duration and severity of involvement of the various systems. Various imaging (diagnostic and invasive) techniques can be used to detect the various manifestations as well as subsequent complications occurring during the course of disease. The following imaging techniques can be utilized for the purpose of evaluating the patients of DM:

- Radiography
- Special investigations
- Ultrasonography (USG) and color doppler study (including echocardiography – ECHO)
- Computed tomography (CT)
- Magnetic resonance imaging (MRI)
- Radionuclide scintigraphy (including single photon emission computed tomography – SPECT)

The role of imaging in assessing the systemic involvement by DM can be well studied in the system-wise manner. However, before we proceed, let us first discuss in short, the classification of diabetes mellitus:

Type I: Insulin-dependent Diabetes Mellitus (IDDM)

Type II: Non-insulin-dependent Diabetes Mellitus or Maturity onset Diabetes (NIDDM or MODY)

Type III: Diabetes Mellitus secondary to multiple causes including chronic diabetes, hemochromatosis, pancreatic hypoplasia, etc.

100 Hounsfield units (HU). Calcium scoring of the coronary arteries can be done using CT scan for the purpose of screening for coronary arteriosclerosis. CT pulmonary angiography may be used to assess the extent of pulmonary arterial hypertension especially if pulmonary thromboembolic phenomenon is suspected.

Metaiodobenzylguanidine (MIBG) imaging has proved useful in detection of the silent ischemic disease in patients with diabetes mellitus as disruption of the cardiac sympathetic innervation leads to increased threshold of pain perception in these patients. Diabetic patients show decreased uptake of MIBG as compared to normal subjects.

DM is associated with arteriosclerosis in the central and peripheral arteries with subsequent narrowing and alterations in the color and spectral flow pattern that can be well evaluated with Doppler studies. Characteristic findings of arteriosclerosis include thickening of intima-media complex (greater than 0.8 mm), irregular intimal surface, increased echogenicity and calcification in walls. There may be formation of atherosclerotic soft (cholesterol-rich, noncalcified) & calcified plaques with subsequent narrowing of the lumen and hemodynamic changes. Color Doppler may show incomplete filling of color in the lumen of arteries while spectral flow may show changes in the pattern of flow in the form of loss of triphasicity in distal arteries with widening of spectral window and decreased peak systolic velocities. Increased systolic velocities may be seen in post-stenotic areas while absence or minimal flow may be seen in the gangrenous areas. Parvus-tardus pattern is characteristic of severely compromised arterial flow usually secondary to severe atherosclerotic changes. Digital subtraction or CT angiography can be used for further assessment, if surgical treatment is being planned. Digital subtraction angiography (DSA) is the gold standard and has the advantage of being converted in to the therapeutic procedure simultaneously. Recently, MR angiography using time of flight & other newer sequences has emerged as a valuable tool in preoperative vascular assessment of patients with compromised renal functions where iodinated contrast medium may be contraindicated (Figures 1-3).

It is well established that DM accelerates the process of arteriosclerosis in patient with peripheral vascular disease due to other causes as well. Such patients may need interventional radiological procedures for relief of their disease. It is very important to achieve a good glycemic control in these patients in perioperative period. Usually, these patients are put on saline and insulin therapy, irrespective of the type of DM.

As DM is associated with increased risk of nephropathy, the subsequent risk of developing contrast-induced nephropathy following a contrast-enhanced study / procedure is higher. Therefore, patients with DM should be screening thoroughly for renal function before being subjected to such procedures. The type of contrast used in such patients should preferably be nonionic, isomolar agents with higher margins of safety in terms of serum creatinine and eGFR values.

In patients with severely compromised renal functions, when contrast studies are contraindicated, noncontrast MR angiography

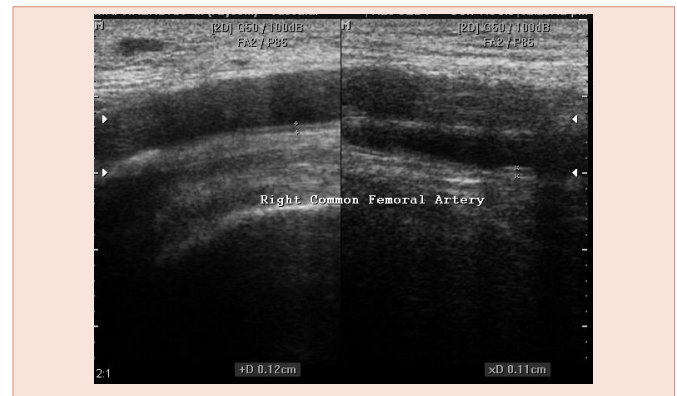


Figure 1: US image shows arteriosclerosis in artery.

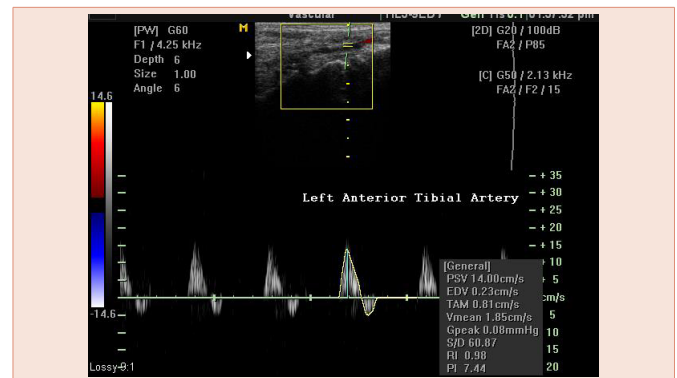


Figure 2: Triplex Doppler image shows microangiopathic changes in distal artery of lower limb.



Figure 3: Triplex Doppler image shows loss of triphasic pattern in arteries in PVD.

plays a pivotal role as mentioned above. It also provides good information about the pathological areas, besides delineating the excellent anatomy, though with acceptable levels of slightly reduced accuracy than contrast-enhanced studies.

Patients with severely compromised renal functions where contrast study is contraindicated but in whom angioplasty is indicated, carbon dioxide (CO₂) gas angiography is an answer. The latter technique utilizes negative contrast created by CO₂ gas. As CO₂

is a natural metabolite in our body and is excreted primarily through lungs, it is considered safer in nephropathy patients.

Urinary system [8,9]

Urinary system manifestations are common and occur primarily in the form of renal involvement followed by involvement of urinary bladder.

The earliest imaging manifestation in diabetic nephropathy is diffuse nephromegaly followed by alteration in parenchymal echogenicity and corticomedullary differentiation as seen on ultrasonography. Initially, the corticomedullary differentiation is accentuated followed by progressive & complete loss of corticomedullary differentiation. Evidence of nephrocalcinosis may be seen as fine clusters or coarse calcifications following the contour of kidney on radiographs, echogenic foci in medullary pyramids or cortex on USG and hyperdense foci on CT scans. On plain radiographs, larger calcifications may reveal central lucency. Renal papillary necrosis may give rise to cortical calcifications, which are otherwise less common than medullary calcifications. In later stages of nephropathy, there is progressive reduction in the size of the kidneys due to nephrosclerosis. Involvement of the renal arteries with subsequent narrowing of lumen results in progressive increase in RI values to more than 0.6 in the main renal & intraparenchymal renal arteries; increase in peak acceleration time; increase in peak systolic velocity & renal artery to aorta velocity ratio. Sometimes, dilatation of pelvicaliceal system may be noted on USG and intravenous urography (IVU) secondary to the obstruction of pelviureteric junction by sloughed papillae. The latter may also lead to delayed and poor functioning of the kidneys. The renal findings are usually bilaterally symmetrical on imaging.

As DM is associated with reduced immunity especially in uncontrolled or poorly controlled cases, it is often associated with secondary infections involving the kidneys. Infections may occur in the form of acute or chronic pyelonephritis, emphysematous or xanthogranulomatous pyelonephritis, renal or perinephric abscess or renal calculi formation especially staghorn type. Acute pyelonephritis is seen as renal enlargement on imaging studies with evidence of spastic pelvicaliceal system on IVU and presence of striated nephrogram on CT urography. Chronic pyelonephritis is seen as scarred kidney with thinned cortex and lobulated contours on IVU, USG or CT. Emphysematous pyelonephritis is characterised by the presence of air within the pelvicaliceal system seen as lucencies on both radiographs and CT scans and as echogenic foci with dirty posterior acoustic shadowing on USG. Xanthogranulomatous pyelonephritis is characterised by enlarged or normal sized kidney with multiple areas of fat & necrosis and often with presence of staghorn calculus. It may mimic tumoral lesion. Renal abscess can be suspected on USG as well-defined or an irregular, focal, necrotic area with posterior acoustic enhancement and peripherally increased vascularity. Perinephric collection displaces and indents the kidney and is better characterised on CT scans as non-enhancing, hypodense collections. Presence of air within the collection is diagnostic of an abscess. Perinephric signs of inflammation are better visualized on MR scans. MRI is also the modality of choice in patients with severely compromised renal functions as significant information can

be obtained even on noncontrast MRI scan of kidneys. CT & MR angiography of renal arteries can be obtained in suspected cases of renal artery stenosis with advantage of avoiding contrast-related side effects & radiation risk in noncontrast MR studies.

Urinary bladder involvement may be seen in the form of usual or emphysematous cystitis. Cystitis is detected on USG by the presence of thickened and irregular walls with residual post-void urine volume. In emphysematous form, air foci may be well documented on plain radiography or CT scans. Diabetic cystopathy occurs late in DM and is characterised by imaging signs of neurogenic bladder on Micturating Cystourethrogram (MCU). The latter reveals high-capacity urinary bladder with smooth and thin walls. But the urinary bladder wall may appear thickened and trabeculated in cases of associated bladder outlet obstruction or cystitis (Figure 4).

Gastrointestinal system [10]

The manifestations of DM in the GIT are usually secondary to autonomic neuropathy. These include alteration in bowel activity which may be in form of delayed peristalsis resulting in gastroparesis, acute non-obstructive gastric dilatation, slow small & large bowel transit resulting in non-obstructive small bowel dilatation and colonic pseudo-obstruction. These conditions can be diagnosed by imaging using a combination of plain radiography and barium gastrointestinal studies that will reveal GIT dilatation with no obvious mechanical obstructive lesion. USG and CT scan of the abdomen in such cases helps in ruling out the other causes of dilatation. Sometimes, DM is associated with intestinal hurry and diarrhoea secondary to autonomic overactivity or presence to malabsorption syndrome. Barium studies are helpful in the latter and show diffuse thickening, coarsening and poor coating of the mucosal folds; flocculation of barium; fragmentation of contrast column and faster intestinal transit. Small bowel enema or barium / CT / MR enteroclysis are better modalities for examination of small bowel but are invasive in nature (Figure 5).

DM mellitus is associated with increased incidence of gastrointestinal infections especially mycobacterial in the Indian

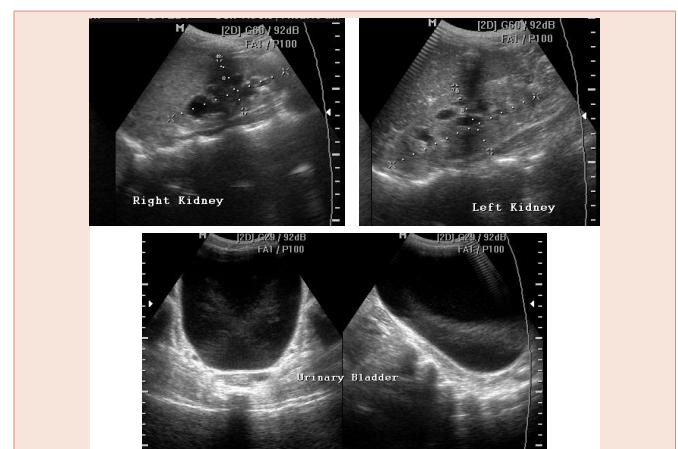


Figure 4 a,b,c: shows Overdistended urinary bladder with bilateral hydronephrosis s/o Neurogenic Bladder with VUR

subcontinent. Barium studies in such cases may reveal presence of mucosal ulcerations, spiculations and angulations of bowel suggestive of adhesions, nonseparable bowel loops and stricture in late stages with proximal dilatation of the bowel loops.

USG and CT abdomen may reveal mesenteric adenopathy with characteristic caseous necrosis on CT; omental / mesenteric nodular thickening; variable bowel wall thickening especially in ileocecal junction and variable ascites.

Hepatopancreatobiliary system [11,12]

Liver involvement in DM is seen on imaging in form of mild to moderate hepatomegaly with varying grades of fatty infiltration. Fatty infiltration of liver is seen as diffuse increase in parenchymal echogenicity on USG and by reduced attenuation values relative to splenic parenchyma on CT scans. MRI may be used to objectively quantitate the fatty infiltration with better analysis of treatment protocol (Figure 6).

Gall bladder (GB) involvement can be in form of dyskinesia secondary to neuropathy. GB may be overdistended due to incomplete emptying. GB dyskinesia can be well documented on USG with preprandial and postprandial volumetric measurements. However, hepatobiliary scintigraphy is more accurate. DM is associated with increased incidence of emphysematous cholecystitis and perforation of GB. CT scan is very accurate in diagnosing these conditions and shows presence of GB wall thickening with presence of mural or intraluminal air with or without pericholecystic fluid or collection and discontinuity of the wall. USG may reveal mural thickening and mural echogenic foci with dirty posterior shadowing. Plain radiographs may show presence of speckled aerocoles in the infrahepatic region corresponding to GB fossa.

DM is commonly associated with fatty infiltration of pancreas secondary to atrophy of pancreatic parenchyma or chronic pancreatitis. Presence of multifocal calcifications and dilated main pancreatic duct may also be noted. Presence of clustered calcification in the midabdomen at the level of D12 and L1 on plain radiograph is highly suggestive of pancreatic origin. Pancreas is best evaluated by CT scan, though USG may be used for screening or follow up of patients with pancreatic disease. Pancreatic ductal disease is better evaluated with magnetic resonance cholangiopancreatography (MRCP) or endoscopic retrograde cholangiopancreatography (ERCP). The former has the advantage of being noninvasive while the latter has the advantage of being simultaneously therapeutic in addition to being diagnostic in nature. Sometimes, congenital anomalies as agenesis of dorsal pancreas may be the cause of DM; hence imaging must be used to rule out secondary DM (Figures 7-9).

Few recent studies have described the fatty infiltration of pancreas as a precursor of diabetes mellitus in obese patients developing NIDDM.

Respiratory system [13,14]

Lungs have been proven by research studies to be the target organ for diabetes induced microangiopathy in type I disease with definite deterioration in lung functions. But in many cases, DM is not associated with any other overt specific manifestation in respiratory



Figure 5: Barium image showing fragmentation and flocculation of contrast s/o malabsorption.

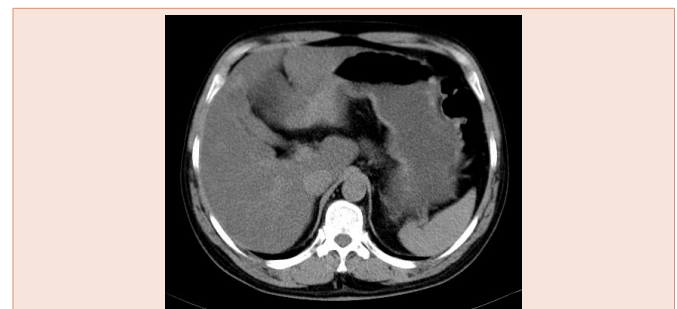


Figure 6: Transaxial CT image diffuse decreased attenuation of hepatic parenchyma relative to spleen s/o diffuse fatty infiltration of liver.

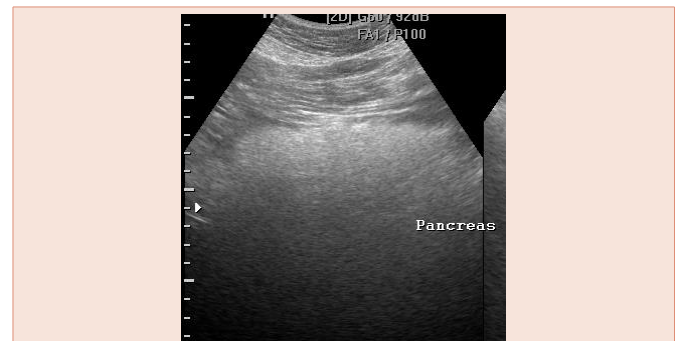


Figure 7: US image shows fatty infiltration of pancreas.

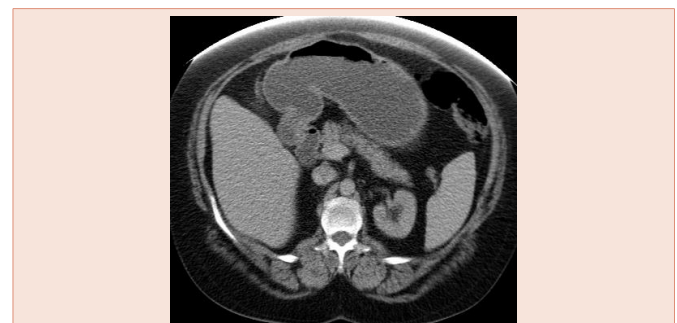


Figure 8: Transaxial CT image shows atrophic fatty pancreas in a patient of IDDM.

system except infections. Patients of DM may develop subsegmental, segmental or lobar consolidation, pleural effusion, tubercular pneumonia, fungal pneumonia, miliary tuberculosis, lung abscess, etc. Consolidation is easily detected on radiograph of the chest as an ill-marginated area of soft tissue opacification with partial or complete obscuration of vascular markings and presence of air bronchogram. In some difficult or complicated cases as tubercular cavity with fungal ball may require further evaluation with CT scan of thorax. CT scan is however, very sensitive in detecting mediastinal and hilar adenopathy especially necrotic nodes (Figures 10,11).

Genital system [8,15]

DM is associated with increased incidence of calcification in the vas deferens and infections especially the Fournier's gangrene (necrotizing fasciitis of penoscrotal region) in males and tubercular tubo-ovarian masses in females. The former is characterised by the presence of air in subcutaneous and fascial planes as seen on plain radiographs or CT scans while the latter are known to be commoner in post-menopausal females. Fournier's gangrene is a true surgical emergency and is associated with high morbidity and mortality. CT scan is the ideal investigation for prompt & accurate diagnosis as well as for the assessment of extent and treatment planning.

DM has been associated with increased risk of carcinoma of endometrium. This can be suspected in early stages as a focal irregular lesion within the endometrial cavity or simply as thickening of the endometrial echo complex on USG. Transvaginal USG has a higher sensitivity than transabdominal USG especially when coupled with color Doppler imaging. MRI of pelvis is also useful in suspicious cases and in detecting early stages with local invasion. Distant spread to lymph nodes and viscera can be equally well evaluated with both CT scan and MRI of abdomen (Figures 12,13).

As DM is associated with increased risk of arteriosclerosis, involvement of penile arteries may lead to impotence. Arterial cause of impotence can be well evaluated with color Doppler study of penile arteries with and without papaverine injection. Impotent patients with arterial cause reveal failure of peak systolic velocities to rise above 25cm/sec following papaverine injection.

Central Nervous system [16,17]

As DM is associated with arteriosclerosis and atherosclerosis, the incidence of cerebrovascular strokes in these patients is relatively higher. Noncontrast CT scan of head is the investigation of choice in these patients. An infarct is seen as a well defined hypodense area often wedge shaped involving both gray and white matter with effacement of the sulcal spaces and mild mass effect. Acute hemorrhage is seen as an ill-defined hyperdense area with surrounding hypodensity producing mild to moderate mass effect. In the first few hours of stroke, MRI brain especially diffusion weighted images are much more sensitive in detecting hyperacute infarcts. Both CT and MR angiography are useful in detecting occlusion of major arteries of brain.

Ischemic demyelination results, when arteriosclerosis involves multiple small arteries supplying the white matter of brain without major occlusion. The latter is seen as diffuse hypodensity of white matter especially in the periventricular region with accentuated



Figure 9: US image shows chronic calcific pancreatitis with intraductal calculi.

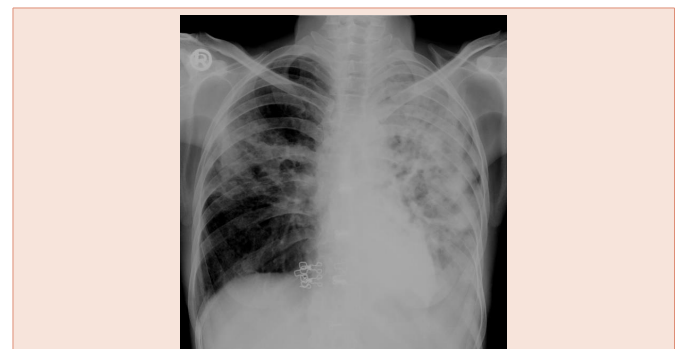


Figure 10: Radiograph of chest shows bilateral Koch's chest with cavitary and cystic changes.

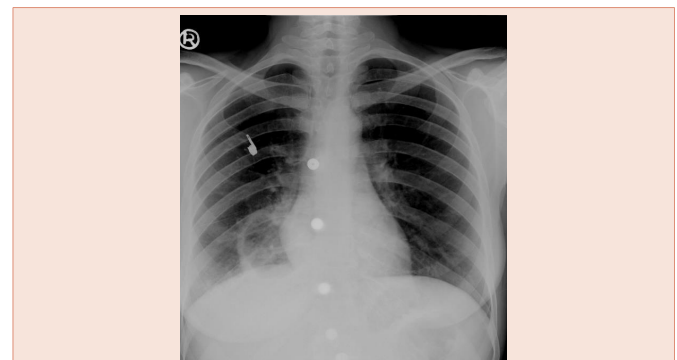


Figure 11: Radiograph of chest shows an abscess in the right lower lobe.



Figure 12: USG scan shows tubo-ovarian mass on left side.

gray white matter differentiation and no obvious postcontrast enhancement or mass effect. MRI is much more sensitive in detecting white matter demyelination revealing diffuse hyperintensity on both T2-weighted and T2-FLAIR images (Figures 14-16).

Visual system [18,19]

DM is associated with multiple manifestations in the visual system including the lens, posterior chamber, retina, optic nerve and visual cortex. Many of these are evaluated by techniques unrelated to the field of radiology.

Although cataract can be evaluated well with ophthalmoscopic examination, nevertheless, loss of anechoic appearance is highly suggestive of cataract on high resolution USG of eye. USG is also very useful in detecting thickening of posterior capsule of the lens. It is the investigation of choice for evaluation of vitreous chamber in patients with opaque anterior chamber or lens. USG can detect vitreous hemorrhage & membrane formation and choroidal & retinal detachment with high accuracy. The latter is seen as thin detached membrane floating in the vitreous chamber of eye attached posteriorly at the optic head and anteriorly at the choroid. Vitreous hemorrhage is seen as hypochoic, ill-defined lesions or as fine internal floating echoes. Proliferative vitreous membranes can be recognised by the presence of color flow on Doppler imaging (Figures 17,18).

Diabetic retinopathy can be well studied with fluorescein angiography. Visual cortex can be studied by CT scan of brain or more sensitively by MRI brain.

ENT region [20]

Patients of DM have increased risk of fungal infections involving the nasal & paranasal sinus (PNS) region, otitis and mastoiditis.

Mucormycosis is seen as a common nasal and PNS infection in DM. as the infection advances, it causes osseous destruction and may involve the roof of the nasal cavities to enter the intracranial cavity. Radiographs of the PNS give limited information in the form of opacification of sinuses and expansion of sinus cavities. High resolution CT scan of the nasal and PNS region give detailed information about the extent of the disease, severity of bony destruction and involvement of vital structures at the skull base. CT demonstrates soft tissue attenuating masses with destruction of bony septae in ethmoid sinuses, nasal septum, osteomeatal unit complex and turbinates with expansion of cavities. Linear internal hyperdensities are characteristic of fungal infection. However, MRI is superior to CT in detecting the intracranial extension of the infection as it can detect meningeal involvement and early edema in the adjacent brain parenchyma. Vascular invasion can be detected well on contrast enhanced images (Figures 19,20).

Patients with DM are at increased risk of developing malignant otitis externa, otitis media and mastoiditis. Otitis externa can be well evaluated by otoscopic examination but radiologic examinations may be needed to assess the true extent of the disease. High resolution CT scan of the temporal bone is the modality of choice for complete assessment of the otitis media and mastoiditis. It may reveal the destruction of the ossicular chain, petrous apex and loss of air within the middle ear and mastoid air cells. Intracranial extension may

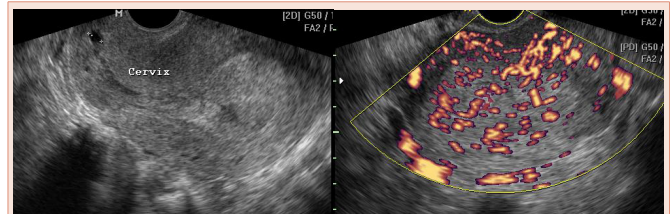


Figure 13a,b: Transvaginal US and Power Doppler scan show carcinoma endometrium.



Figure 14: CT scan image shows MCA territory infarct on left side.

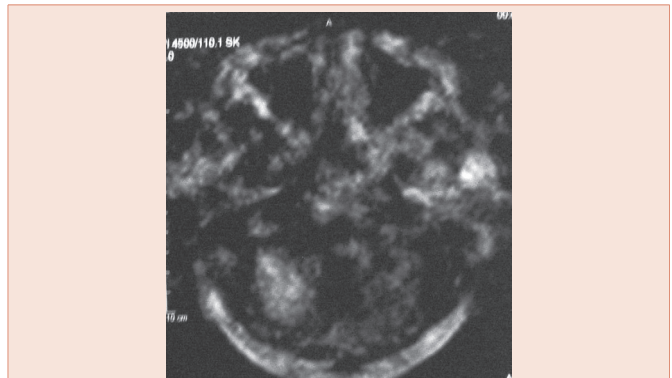


Figure 15: Diffusion weighted MR image shows hyperacute right cerebellar infarct.

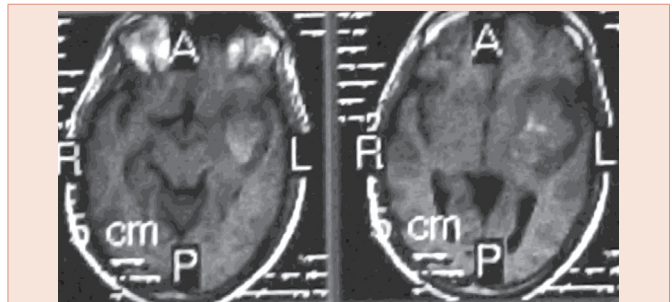


Figure 16: T1-weighted MR images show subacute phase of ICH in left temporal lobe.

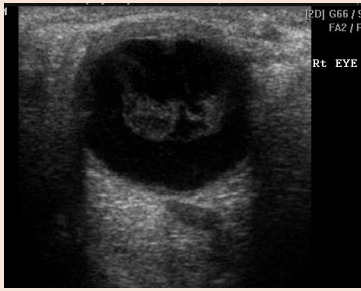


Figure 17: US image shows hyperplastic vitreous exudates in DM patient.

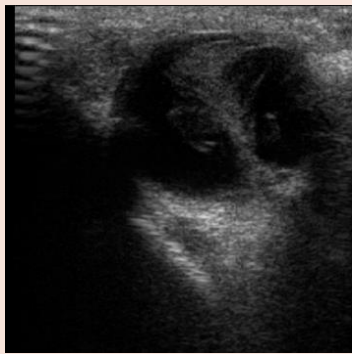


Figure 18: US image shows retinal detachment.



Figure 19: Transaxial CT image shows osteomyelitis of right antral floor secondary to apical dental infection in a DM patient.



Figure 20: Coronal CT image in a patient of fungal polyposis.

be seen in the form of destruction of the sinus tympani or tegmen tympani bone. MRI is superior in detecting the meningeal or cerebral involvement. Lateral oblique views of mastoid may be used to detect the opacification of the mastoid air cells and destruction of the tegmen.

Musculoskeletal system [21,22]

The commonest manifestation of DM in the musculoskeletal system is increased incidence of infections. This may be seen in the form of swelling of soft tissues with or without abscess formation with or without presence of aerocoles secondary to anaerobic infection or communication with external environment. Soft tissue swelling is detected by the effacement of fat planes in radiographs with internal lucencies due to presence of air. USG is able to detect the soft tissue edema as increased echogenicity in soft tissues with presence of pavement like pattern in the subcutaneous tissues. Abscess is seen as a thick-walled, hypochoic collection with posterior acoustic enhancement showing internal septations & debris and presence of inflammatory pattern of vascularity at the periphery on color Doppler imaging. MRI can also detect edema of soft tissue and abscess formation as hyperintensity on T2W images.

Osteomyelitis occur either secondary to contiguous spread from soft tissue infection or by hematogenous spread. The earliest investigation that can detect osteomyelitis is radionuclide scanning that reveals an area of increased radiotracer uptake. MRI can reveal early osteomyelitis as an area of hyperintensity within the bone on STIR images with sub-periosteal or parosteal fluid collection but slightly later than scintigraphy. USG can detect osteomyelitis by the presence of subperiosteal or parosteal fluid collection in the long bones and presence of inflammatory pattern of vascularity on color Doppler imaging. Plain radiographs and CT scans are useful in detecting when osteomyelitis is usually well developed and is seen as an area of osseous destruction with formation of abscess in adjacent soft tissues and sinus, cloacae or sequestrum formation in chronic stages. CT and MRI are complementary in cases of osteomyelitis (Figures 21-23).

Neuropathic foot is a known complication of diabetes mellitus seen secondary to peripheral nervous system involvement. Neuropathic foot is characterised by increased density of bones that are disintegrated & fragmented resulting in permanent deformities at joint (subluxation or dislocation). Acro-osteolysis and soft tissue calcification may be present. In childhood, neuropathic foot may be associated with retarded bone age.

Gestational diabetes mellitus (GDM) [23]

The discussion about role of imaging in diabetes mellitus is incomplete, if we do not discuss the role of imaging in GDM. Diabetes mellitus occurring during the course of pregnancy not only affects the maternal systems but also affects the fetus and perinatal outcome.

GDM is associated with an increased risk of urinary tract infections especially pyelonephritis and antepartum eclampsia. The role of imaging in the former has already been discussed; however emphasis should be on minimizing the radiation exposure to the

fetus. Eclamptic patients may require CT scan of the head in case of neurologic manifestations. CT scan may reveal presence of hemorrhagic venous infarcts and dural venous sinus and cerebral venous thrombosis. In some patients, ischemic changes are limited in the white matter of the occipital lobes that are better visualised on MRI brain.

Antenatal complications of GDM depend upon the gestational age at which the GDM sets in. Majority can be easily detected on antenatal USG and include polyhydramnios, thickened placenta, accelerated placental maturity, large fetal weight and increased risk of congenital anomalies especially congenital heart disease, renal anomalies and musculoskeletal anomalies especially caudal regression syndrome. Complex spinal anomalies may require further evaluation with fetal MRI (Figure 24).

GDM is also responsible for multiple postnatal complications in the neonate. These include prematurity, hyaline membrane disease of lungs and failure to thrive. Hyaline membrane disease manifests in the form of decreased inflation of lungs followed by fine diffuse nodularity, diffuse consolidation and subsequently classical *white-out lungs* (Figure 25).

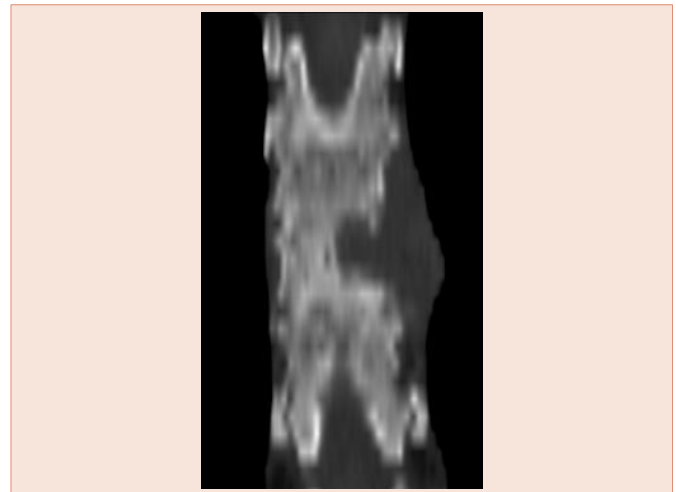


Figure 23: Coronal CT MPR image shows Pott's spine.

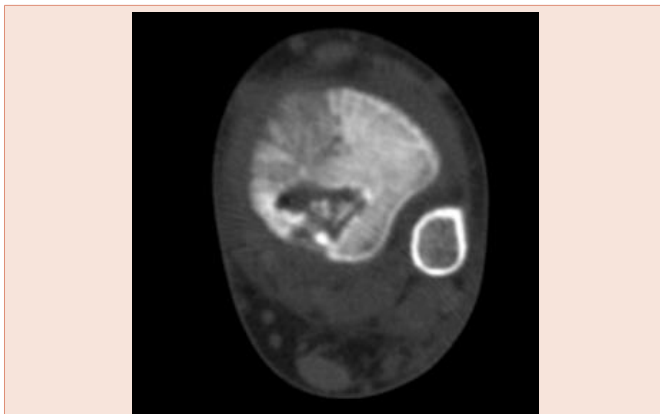


Figure 21: Transaxial CT image shows osteomyelitis of tibia with sequestrum formation.



Figure 24 a,b: shows Grade II-III placenta with thickening in second trimester in a patient with gestational DM.



Figure 22: CT sinogram image shows sinus track leading in to the osteomyelitic femur.



Figure 25: AP radiograph of chest shows HMD in a neonate born to a diabetic mother.



References

1. Goraya TY, Leibson CL, Palumbo PJ, Weston SA, Killian JM, et al. (2002) Coronary atherosclerosis in diabetes mellitus: a population-based autopsy study. *J Am Coll Cardiol* 40: 946–953.
2. Miller TD, Rajagopalan N, Hodge DO, Frye RL, Gibbons RJ (2004) Yield of stress single photon emission computed tomography in asymptomatic patients with diabetes. *Am Heart J* 147: 890–896.
3. Mohan V, Ravikumar R, Shanthi Rani S, Deepa R (2000) Intimal medial thickness of the carotid artery in South Indian diabetic and non-diabetic subjects: The Chennai Urban Population Study (CUPS). *Diabetologia* 43: 494–499.
4. Langer A, Freeman MR, Josse RG, Armstrong PW (1995) Metaiodobenzylguanidine imaging in diabetes mellitus: assessment of cardiac sympathetic denervation and its relation to autonomic dysfunction and silent myocardial ischemia. *J Am Coll Cardiol* 25: 610–618.
5. Dyet JF, Nicholson AA, Ettles DF (2000) Vascular imaging and intervention in peripheral arteries in the diabetic patient. *Diabetes Metab Res Rev* 16: S16–S22.
6. Ahluwalia AI, Bedi VS, Indrajit IK, Souza JD (2003) Evaluation and Management of Peripheral Arterial Disease in Type 2 Diabetes Mellitus. *Int J Diab Dev Ctries* 23: 61–65.
7. Toprak o, Cirit M (2006) Risk Factors for Contrast-Induced Nephropathy. *Kidney Blood Press Res* 29: 84–93.
8. Rodriguez-de-Velasquez A, Yoder IC, Velasquez PA, Papanicolaou N (1995) Imaging the effects of diabetes on the genitourinary system. *Radio Graphics* 15: 1051–1068.
9. Özlem T, Hüsnü T, Eda E, Şule D, Enis Y (2008) Correlation of Renal B-Mode Ultrasonographic Findings with Diabetic Nephropathy Stage. *Marmara Medical Journal* 21: 112–117.
10. Wolosin JD, Steven V. Edelman (2000) MD Diabetes and Gastrointestinal Tract. *James D. Clinical Diabetes* 18.
11. Singh S, Chander R, Singh A, Mann S (2006) Ultrasonographic evaluation of gall bladder diseases in diabetes mellitus type 2. *Indian J Radiol Imaging* 16: 505–508.
12. Farrell FJ, Keeffe EB (1998) Diabetes and the hepatobiliary system. *Clinics in liver disease* 2: 119–131.
13. Goldman MD (2003) Lung dysfunction in Diabetes. *Diabetes Care* 26: 1915–1918.
14. Farquhar I, Farquhar I, Summers KH, Sorkin A, Weir E (2002) Concomitant Respiratory Disease in Diabetes: Trends in Health Outcomes. *Abstr Acad Health Serv Res Health Policy Meet* 19: 14.
15. Levenson RB, Singh AK, Novelline RA (2008) Fournier Gangrene: Role of Imaging. *RadioGraphics* 28: 519–528.
16. Selvarajah D, Tesfaye S (2006) Central nervous system involvement in diabetes mellitus. *Current Diabetes Reports* 6: 431–438.
17. Lukovits TG, Mazzone T, Gorelick PB (1999) Diabetes mellitus and Cerebrovascular Disease. *Neuroepidemiology* 18: 1–14.
18. Kleinmann G, Hauser D, Schechtman E, Landa G, Bukelman A, et al. (2008) Vitreous hemorrhage in diabetic eyes previously treated with panretinal photocoagulation. *Internation Ophthalmology* 28: 29–34.
19. Larkin GL (2007) Retinal Detachment. (<http://emedicine.medscape.com/article/798501-overview> as updated on April' 2007)
20. Bhadada S, Bhansali A, Reddy KSS, Bhat RV, Khandelwal N, et al. (2005) Rhino-ocular-cerebral mucormycosis in type 1 diabetes mellitus. *Indian Journal of Pediatrics* 72: 671–674.
21. Cunha BA (2008) Diabetic foot infections. (<http://emedicine.medscape.com/article/237378-overview> as updated in June' 2008)
22. Mishra N, Saran D, Charles C, Abdel-Hadi AH (2008) Pyogenic vertebral osteomyelitis in well-controlled type-II DM. *Practical Diabetes International* 25: 70.
23. Moore TR (2014) Diabetes mellitus and Pregnancy. (<http://emedicine.medscape.com/article/127547-overview>)

Copyright: © 2016 Rastogi R, et al. This is an open-access article distributed under the terms of the Creative Commons Attribution License, which permits unrestricted use, distribution, and reproduction in any medium, provided the original author and source are credited.

Citation: Rastogi R, Jain SK (2016) Imaging in Diabetes Mellitus. *Arch Clin Nephrol* 2(1): 017–025. DOI: <http://dx.doi.org/10.17352/acn.000009>